ADVANCED MATERIALS INTERFACES
www.advmatinterfaces.de

Tuning of Smart Multifunctional Polymer Coatings Made by Zwitterionic Phosphorylcholines

Alexander S. Münch, Stefan Adam, Tina Fritzsche, and Petra Uhlmann**

In the last years, the generation of multifunctional coatings has been moved into the focus of interface modifications to expand the spectrum of material applications and to introduce new smart properties. Herein a promising multifunctional and universally usable coating with simultaneous antifouling, easy-to-clean, and anti-fog functionality is presented based on smart polymer films consisting of copolymers with 2-methacryloyloxyethyl phosphorylcholine (MPC), realizing the function of the film and photoreactive 4-benzophenyl methacrylate (BPO), which is responsible for stability and crosslinking. The easy-to-clean effect is demonstrated qualitatively and quantitatively by oil droplet detachment experiments. The antifouling behavior against different germs is investigated by cell adhesion experiments. Furthermore the anti-fog performance is shown by breathing on the surfaces. To study the influence of the different amounts of copolymerized BPO, the grafted films are characterized by atomic force microscopy (AFM), infrared spectroscopy (ATR-FTIR), as well as contact angle measurements. In situ spectroscopic ellipsometry is performed to investigate the swelling behavior of the thin films as a function of the time of UV-irradiation. It is found that a degree of swelling of 15 and a water contact angle of less than 12° are the key parameters necessary for the generation of multifunctional coatings.

1. Introduction

Products with a higher value and consumer acceptance can be created by implementation of multifunctional coatings.[1–3] This type of surface modification combines different functionalities, e.g., anti-ice,[4–6] easy-to-clean,[7–9] anti-fog,[10–12] and antifouling[13–15] in the same layer. The surface modification by grafting and crosslinking of polymer chains is an effective methodology to control and tailor surface properties of the bulk substrate, such as wettability, adhesion, and friction. However, most of the presented smart polymer coatings exhibit only one of the above-mentioned functionalities. Therefore, a further tailoring of the known functional polymers or the development of new materials or strategies is required.

Recently, polymers with zwitterionic groups, like phosphorylcholine, carboxybetaine, or sulfobetaine groups, were synthesized and their films investigated for example, antifouling and easy-to-clean applications. Among these this group of polymers with an inner-salt structure 2-methacryloyloxyethyl phosphorylcholine is a promising and quite well studied representative.[16] This macromolecule contains a zwitterionic phosphorylcholine group composed of a positively charged trimethylammonium cation and a negatively charged phosphate anion. Because of this structure, which also appears as the head group of phospholipids of the cell membrane, 2-methacryloyloxyethyl phosphorylcholine (MPC) and its copolymers are considered as biocompatible[17,18] with a lower cytotoxicity compared to other polymers, as, e.g., polyethylene glycol (PEG).[19] Because of its bioinertness as a result of impaired electrostatic interactions and the high degree of swelling connected with a high content of highly mobile water molecules around the phosphorylcholine group,[20–24] MPC is intensively investigated for biosensing applications,[25] for bioconjugation on nanocolloids,[26] for anti-fog and self-cleaning material,[27,28] as protein repellent,[29,30] as well as antifouling polymer.[30–34] Furthermore applications in the field of chromatography[35,36] and oil–water separation membranes with oil-repellent properties were demonstrated.[37]

In addition to its functionalities MPC has a reactive methacrylate group, which makes it accessible for a variety of different polymerization techniques with numerous monomers based on methacrylates.[24,33,38,39] To explore the grafting of MPC on various substrates under mild conditions, like room temperature, photoreactive monomers, such as 4-benzophenyl methacrylate (BPO), can be used as anchor and crosslinking agent. The aromatic keto group of benzophenone can create a biradical under low-intensity UV irradiation (254–365 nm). It can abstract hydrogens from a suitable C—H hydrogen donor bond. The hydrogen atom of these bonds is abstracted by the biradical triplet excited state of the benzophenone induced by UV-light resulting in a new C—C bond,[40,41] without UV

Dr. A. S. Münch, Dr. S. Adam, T. Fritzsche, Dr. P. Uhlmann
Leibniz-Institut für Polymerforschung Dresden e.V.
Hohe Straße 6, D-01069 Dresden, Germany
E-mail: muench@ipfdd.de; uhlmannp@ipfdd.de
Dr. P. Uhlmann
Department of Chemistry
Hamilton Hall
University of Nebraska-Lincoln
639 North 12th Street, Lincoln, NE 68588, USA
The ORCID identification number(s) for the author(s) of this article can be found under https://doi.org/10.1002/admi.201901422.

DOI: 10.1002/admi.201901422

oxidative damage of the polymer or the substrate.[42] The potential of this grafting procedure was recently demonstrated for different fields of application[43–46] as well as for various substrates.[47–51] The usage of benzophenone as an anchor and crosslinking agent is a universally usable principle for application-oriented coating processes.

In this study, we present a new multifunctional polymer coating combining the zwitterionic 2-methacryloyloxyethyl phosphorylcholine unit as the functional group and the photoreactive 4-benzophenyl methacrylate used for a fast one-step deposition and crosslinking process by UV-irradiation. Complementary to our previously published studies regarding easy-to-clean and antifouling coatings made by MPC-layers on foils and cellulose, which are highly application oriented with the focus on the adaption of a thin film forming process from the lab to a technical coating process,[28,30,31] here a fundamental study of the involved structure–property relationships will be presented, which includes an investigation of the influence of polymer composition and grafting parameters on the properties of the obtained coatings and their performance. In previous studies, co-polymers of MPC and glycidyl methacrylate as well as MPC and BPO were prepared by free radical polymerization.[30,31] In this study, for a better control of the constitution and the physical properties, MPC-co-polymers with different contents of BPO were synthesized by atom transfer radical polymerization (ATRP). The investigated copolymers, synthesized by using MPC and 4-benzophenyl methacrylate for the first time, combine antifouling, anti-fog, as well as easy-to-clean properties. The presented work demonstrates the relevance of a balanced ratio between the functional and the anchor unit. Therefore, a series of three new copolymers with different amounts of BPO was synthesized to study the influence of crosslinking, swelling behavior, and wettability on the multifunctionality by in situ spectroscopic ellipsometry, contact angle (CA) measurements, and FTIR-spectroscopy. With this systematic investigation a general statement regarding the tunability and the mechanism of antifouling, easy-to-clean, and anti-fog properties is possible, at which the influence of BPO-content and UV-irradiation time on the successful preparation of a multifunctional coating will be extracted for the first time. It will be shown that the chemical composition of the polymer, the degree of crosslinking, as well as thin film properties like thickness, degree of swelling, and wettability are crucial for the adjustment of the film function. The study will also demonstrate a universal coating principle for the functionalization of commonly used organic as well as inorganic substrates.

2. Results and Discussion

2.1. Preparation and Surface Properties of Thin MPC Layers on SiO_2

The new zwitterionic MPC-copolymers with different ratios of the crosslinker 4-benzophenyl methacrylate were synthesized as random copolymers by ATRP, as demonstrated in Scheme S1b (Supporting Information). This is in contrast to published copolymers composed of more than two different monomers or using another benzophenone monomer generated by radical polymerization.[34,52–54] To investigate the mechanism behind the easy-to-clean, anti-fog, and antifouling effect as well as to determine the optimal composition for these applications, copolymers with monomer feed ratios ([MPC]:[BPO]) of [198]:[2] (≙ 1% BPO), [195]:[5] (≙ 2.5% BPO), and [190]:[10] (≙ 5% BPO) were prepared. The compositions were confirmed by ^{1}H-NMR spectroscopy (see the Supporting Information) and consisted of [99]:[1] (≙ 1% BPO),[49]:[1] (≙ 2% BPO), and [431]:[19] (≙ 4.2% BPO), which approximately matched the monomer feed ratios. Due to the high amount of the zwitterionic MPC-units, which is responsible for the particular properties resulting in the three fields of application mentioned above and discussed in detail below, all polymers are very hydrophilic. The benzophenone group in the BPO-comonomer can abstract hydrogens from a suitable hydrogen donor by forming a biradical triplet excited state of the benzophenone induced by UV-radiation resulting in new C—C bonds.[40,41,55] This crosslinking and anchor group is an attractive unit in functional polymers, because an oxidative damage of polymer and substrate can be avoided. Furthermore a very fast one-step generation of a thin film under mild conditions, like room temperature, is possible, whose kinetics was investigated previously.[6,31]

The transition states of the electrons of the prepared $MPC_{1\%}$, $MPC_{2\%}$, and $MPC_{4\%}$ polymers were investigated by UV–vis spectroscopy. The corresponding spectra are demonstrated in **Figure 1** in comparison to the pure MPC-polymer (in ethanol) without any benzophenone methacrylate and the pure BPO-polymer (in chloroform). They indicate a broad and intensive band with a maximum between 274 nm for $MPC_{1\%}$ and 288 nm for $MPC_{4\%}$. The band of $MPC_{2\%}$ (283 nm) can be detected between the other two bands. That means, the adsorption depends on the BPO content and shifts to a higher wavelength with an increasing amount of BPO. This observation can be verified by the spectra of the pure MPC polymer with a maximum at 245 nm and of pure BPO with an adsorption band at 299 nm. Both polymers were synthesized by ATRP of the corresponding methacrylates. The intensive bands of the copolymers are a result of the overlap of the π→π* transitions of the C=O bands of the methacrylate motif on the one hand and the π→π* transitions of the aromatic rings of the benzophenonic units one the other hand, indicated by a fronting behavior of the peak shape. In the case of the pure MPC-polymer no aromatic rings are

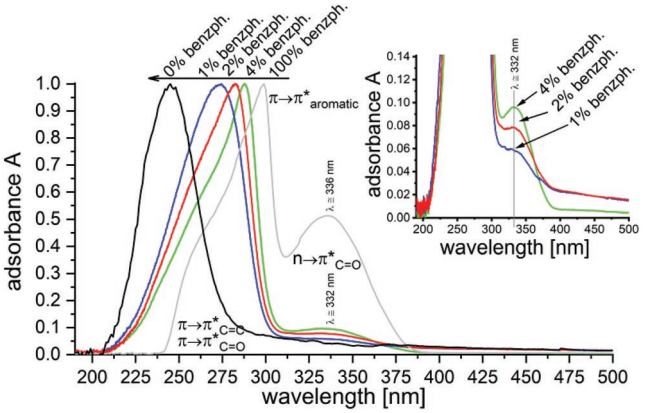

Figure 1. UV–vis spectra of the investigated polymers $MPC_{1\%}$ (blue), $MPC_{2\%}$ (red), and $MPC_{4\%}$ (green) in comparison with the spectra of the pure MPC-polymer (black) and of the pure BPO-polymer (gray).

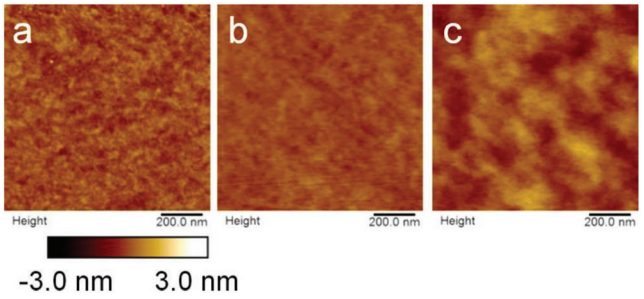

Figure 2. a) AFM-images of $MPC_{1\%}@SiO_2$, b) $MPC_{2\%}@SiO_2$, and c) $MPC_{4\%}@SiO_2$. The scale bar correlates with 200 nm and the scan size was 2 × 2 µm.

present in the polymer resulting in a relatively symmetric band, because no additional electron transition beside the C=O bond appears. The two different π→π* transitions are clearly detected for the pure BPO-polymer illustrated by a significant shoulder of the adsorption band. Beside this adsorption band a typical band of $n\rightarrow\pi^*$ transitions corresponding to the ketyl group of the benzophenone structure can be detected at ≈335 nm. The value of the peak area depends on the amount of the BPO in the polymer. The area decreases with decreasing amount of BPO in the prepared copolymers, shown in the insert of Figure 1.

Based on these results the films of the MPC polymers were prepared by a single step deposition approach using an UV-lamp irradiation with a nominal wavelength of 254 nm and different crosslinking times between 30 s and 11 min, because previous experiments with UV-lamps with other wavelengths like 365 nm were not successful. It seems that the applied lamp denoted with 254 nm emits UV-light with a relative broad wavelength range and covered a spectral range in which all significant groups of benzophenone (the intensive π→π* and the weak $n\rightarrow\pi^*$ adsorption bands) adsorbate. In the first step the stability and homogeneity of the prepared films was investigated. The atomic force microscopy (AFM) images shown in **Figure 2** demonstrate very homogenous and smooth layers without any holes with low S_q values of 0.355 nm for $MPC_{4\%}@SiO_2$, 0.164 nm for $MPC_{2\%}@SiO_2$, and 0.246 nm for the $MPC_{1\%}@SiO_2$ film. The homogeneity of the films and the absence of any holes are essential prerequisites for a uniform and reproducible performance also at extended surfaces.

Silicon wafers with a native SiO_2 thickness of 1.3 nm were used as substrates for the $MPC_{x\%}$ layers because of its physical and chemical homogeneity as well its reflective properties, which enables access to optical investigation methods such as ellipsometry. However, the absence of any C—H bonds on purified silicon surfaces is the problem of this substrate in the context of the preparation of $MPC_{x\%}$ film by grafting via benzophenone groups. Therefore, intensive studies regarding the stability behavior were performed by comparing the thicknesses of the dry film direct after the crosslinking reaction and extraction of the substrates with a good solvent for the $MPC_{x\%}$ polymer, like water or ethanol, after 30 min and 24 h. 24 h were chosen because this time is comparable with the cultivation time in cell adhesion experiments and much larger than the time-consuming in situ ellipsometric analyses of the film swelling behavior, which needed ≈2 h. The corresponding results are illustrated in Figure S4 of the Supporting Information and the expected decrease of the film thickness after 30 min extraction due to the removal of un-crosslinked polymer. Since the layer thicknesses did not change after 24 h of extraction, the films were stable against the used solvents. This result can be attributed to strong electrostatic interactions between the zwitterionic MPC units and the cleaned and plasma activated SiO_2 surface of the silicon wafer. Additionally, the benzophenone units crosslink the polymer chains among each other resulting in a higher stability of polymer film in comparison to films without any benzophenone. The usage of crosslinking agents is a widely used method to improve the stability of adsorbed films.[56–58] The used SiO_2 surface is a model substrate and was selected to investigate the effects of MPC regarding to anti-fouling, easy-to-clean, and anti-fog properties fundamentally. Recently published studies have shown the potential of MPC-BPO copolymers for various organic substrates, such as cellulose and foils.[28,31] In these cases the formed ketyl radicals can insert in C—H bonds of the substrates and anchor the polymer chains covalently on the surface.

The film formation process was investigated by FTIR-spectroscopy by using the un-crosslinked $MPC_{x\%}$-polymer film (black curve) as a reference for the films, which were crosslinked for 1 min (red) and 11 min (blue). The spectra of the $MPC_{4\%}@SiO_2$ films are demonstrated exemplary in **Figure 3**. The corresponding analytical results for $MPC_{1\%}$ and $MPC_{2\%}$ layers are summarized in Section S3 of the Supporting Information. In the infrared spectra the typical vibrational bands of the $MPC_{x\%}$ polymer can be detected. Beside the intensive carbonyl band at 1722 cm^{-1} of the methacrylate structures of the polymer backbone the stretching vibrations of the $N^+(CH_3)_3$ group at 1483 cm^{-1} and the P=O unit at 1237 cm^{-1} can be found. The band which indicates the carbonyl vibration of the diarylketo group of the benzophenone unit is detectable at 1662 cm^{-1}. By evaluating qualitatively, the areas of this band in the three spectra of Figure 3 the crosslinking reaction can be monitored. The area in the spectra of the ungrafted polymer is higher than the respective areas after crosslinking. The areas decrease with increasing irradiation time as a result of the decreasing amount of active C=O groups of the benzophenone. A higher amount of ketyl radicals was formed which can react with C—H bond

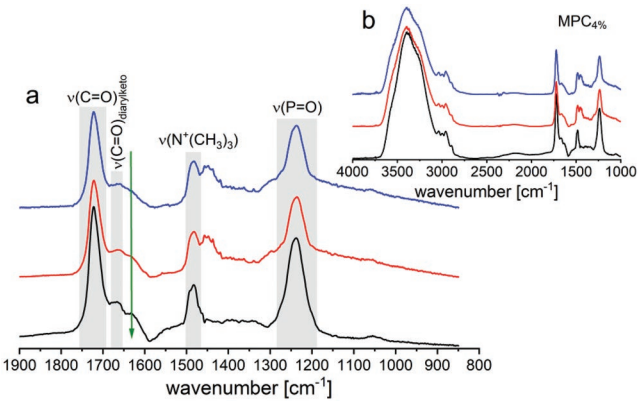

Figure 3. FTIR-spectra of the spin coated, un-crosslinked $MPC_{4\%}@SiO_2$ (black) in comparison to the crosslinked layer after 1 min irradiation (red) and 11 min irradiation (blue) a) in detail and b) as overview spectra.

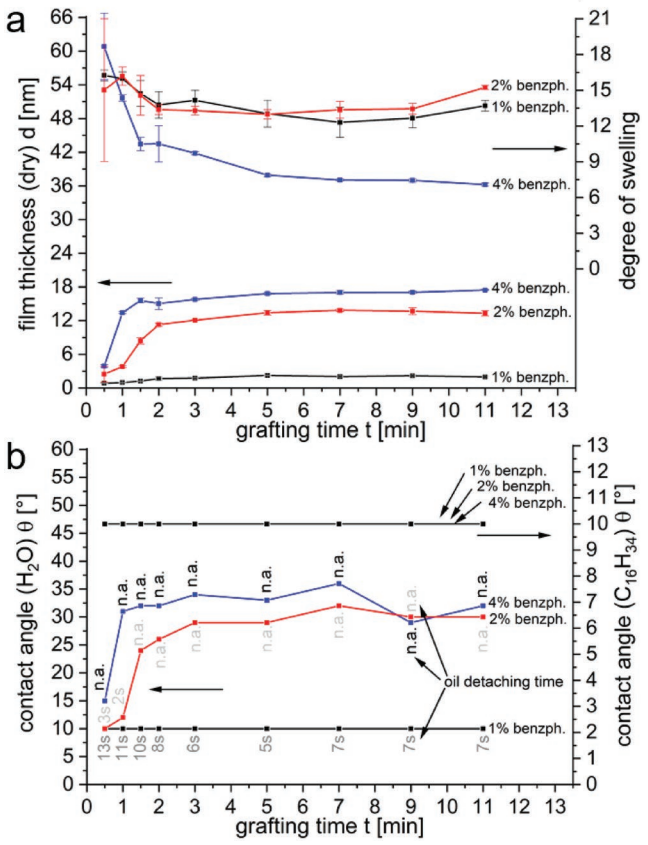

Figure 4. a) Results of the investigation of the film thickness and the corresponding degree of swelling depending on the grafting time of $MPC_{1\%}@SiO_2$ (black), $MPC_{2\%}@SiO_2$ (red), and $MPC_{4\%}@SiO_2$ (blue) determined by spectroscopic in situ ellipsometry and b) of water as well as hexadecane contact angles of $MPC_{1\%}@SiO_2$ (black), $MPC_{2\%}@SiO_2$ (red), and $MPC_{4\%}@SiO_2$ (blue). The numbers indexing every measuring point in b) denote the oil detaching time in seconds. n.a. means that the oil droplet had not stripped off within 1 min.

to form new bonds. That means that the degree of crosslinking increases with increasing irradiation time. The spectra of the $MPC_{1\%}$ and $MPC_{2\%}$ polymers (see the Supporting Information) demonstrate the same trend.

Since the time of irradiation, denoted as grafting time, has an influence on the degree of crosslinking, the impact of the crosslinking time on the resulting dry film is demonstrated in **Figure 4**a. The curves of the different $MPC_{x\%}$ polymers indicate a decreasing film thickness with decreasing amount of BPO units in the polymer. After 11 min the film thickness of $MPC_{1\%}@SiO_2$ is 2.0 nm, of $MPC_{2\%}@SiO_2$ is 13.3 nm, and of $MPC_{4\%}@SiO_2$ is 17.5 nm for instance. Because of the lower amount of BPO in $MPC_{1\%}$ in comparison to the other polymers fewer ketyl radicals can be formed, the degree of crosslinking is smaller and more MPC-polymer can be extracted by ethanol, resulting in a much smaller film thickness. Furthermore, the film thicknesses become maximal after a grafting time of ≈2 min. In this time all crosslinking points which are necessary for the film generation are formed and the film thicknesses do not increase further.

Because of the zwitterionic structure of MPC the copolymers are very hydrophilic molecules, resulting in a good solubility and high swelling in water. The degree of crosslinking caused by the BPO units has an influence on the degree of swelling, as presented in Figure 4a. The polymer with the highest BPO-content ($MPC_{4\%}$) exhibits the largest film thickness because of the higher amount of crosslinking points. Besides, the polymer chains are more densely interconnected among each other, resulting in a lower degree of swelling of 7.0 in comparison to values of 15.2 for $MPC_{2\%}$ and 13.6 for $MPC_{1\%}$ (each film was prepared by irradiation for 11 min). A similar influence has the irradiation time. With increasing grafting time, the points of crosslinking increase, leading to a decreasing degree of swelling up to 2 min of grafting time in the case of $MPC_{1\%}$ and $MPC_{2\%}$, which correlates excellently to the increase in the dry film thickness. After this time the swelling degree is constant. In the case of MPC with the highest BPO content, the plateau of the degree of swelling is reached at grafting times longer than 5 min because of stronger post crosslinking after film formation.

2.2. Analysis of Anti-Fog Effect

To study the anti-fog performance of the synthesized polymers, thin films on glass substrates were prepared with the same condition as at silicon wafers and with an UV-irradiation time of 1 min. Afterward, the as-prepared films are breathed on, whereas uncoated glasses are used as reference. The results are qualitatively evaluated and demonstrated for $MPC_{1\%}$, $MPC_{2\%}$, and $MPC_{4\%}$ in **Figure 5**. All functionalized glasses show an excellent anti-fog performance. This effect is attributed to the very hydrophilic behavior of the betaine structure of the MPC. The contact angles of the corresponding layers are very low ($MPC_{1\%} < 10°$, $MPC_{2\%} < 12°$, $MPC_{4\%} < 31°$), but increase with a larger amount of BPO resulting in a higher degree of crosslinking. In contrast to the uncoated glasses the water droplets of the breath do not form droplets with a defined shape and spread completely on

Figure 5. Visual demonstration of the anti-fog effect of a) $MPC_{4\%}@SiO_{2(glass)}$, b) $MPC_{2\%}@SiO_{2(glass)}$, and c) $MPC_{1\%}@SiO_{2(glass)}$. The images present in each case the comparison of a coated glass sample (upper slide) with a nonfunctionalized one (lower slide).

the surface. Because the diffuse reflection of light is prevented it is possible to look through coating and glass. The high degree of swelling assists this effect by forming a thick water layer on the surface (thick in comparison to the dry film) when the water molecules of the breath adsorb and penetrate the polymer films. The increasing water contact angle caused by a higher amount of BPO has obviously no negative effect on the anti-fog performance.

2.3. Investigation of Easy-to-Clean Effect

To evaluate the easy-to-clean behavior of the different $MPC_{x\%}$-films quantitatively the oil repellency was determined by so-called "oil droplet detachment experiments," inspired by the experiments of He et al. concerning membranes with oil–water separation properties.[37] Thereby a droplet of oil was prepared on the $MPC_{x\%}$-films. Afterward the substrates were immersed into pure water and the time of oil-detachment was measured. The oil-detachment times are mentioned as numbers in Figure 4b at the curves describing the water contact angle. When no detachment was observed within 1 min the easy-to-clean effect was assessed as negative and denoted with n.a. A typical experiment is illustrated in **Figure 6**. It is noticeable that the $MPC_{4\%}$ layer did not show oil-removing properties regardless of the time of irradiation. Furthermore, if the content of benzophenone in the functional polymer is decreased to a value of 1% a very fast oil detachment between 7 and 13 s can be observed independently of the time of irradiation. To understand these phenomena the polymer $MPC_{2\%}$ was investigated in more detail. The experiments show that the oil droplet only removes from the surface when the irradiation time is set to not more than 0.5 or 1 min, respectively. The reason for this behavior obviously is the evolution of degree of swelling and water contact angle with the amount of copolymerized BPO and the irradiation time.

As already described above, the degree of swelling of the polymer films decreases and the water contact angle increases with increasing BPO-content and irradiation time, because of the higher amount of active ketyl radicals resulting in a higher amount of crosslinking points. It seems that the degree of swelling has a direct influence on the oil detachment. If the film does not swell enough, like in the case of the $MPC_{4\%}$ layer when crosslinked more than 90 s, the oil cannot be repelled from the surface. However, the degree of swelling alone cannot explain the oil detachment from $MPC_{2\%}$ films after 1 min and the non-detachment after 2 min of irradiation. Because the degree of swelling is approximately the same after an irradiation time of around 1 min for all three samples, it seems that the water contact angle is the second important factor that influences the easy-to-clean effect. In the case of the $MPC_{1\%}$ films the contact angle is below 10° for every grafting time and the oil detaches from the surface regardless of the time of irradiation. The contact angle of $MPC_{2\%}$ films is also very low (below 12°) after the first 60 s of irradiation and the oil droplet detaches. Starting from 1 min of irradiation the contact angle increases significantly to a value of more than 25° resulting in an absence of the easy-to-clean behavior. The $MPC_{4\%}$ layers show a similar effect, however the starting contact angle after 30 s of irradiation is already 15° and increases to a value of ≈30°. That means, the contact angle is too large, despite the high degree of swelling, for a successful oil detachment. In summary, the right balance between water contact angle and degree of swelling caused by the amount of copolymerized BPO and irradiation time is necessary for reaching the easy-to-clean effect. For the demonstrated polymers a degree of swelling of about 15 in combination with a contact angle below 12° was found to be necessary to generate a surface coating with oil-removing properties.

Based on these results a hypothesis about the mechanism of the oil repellency is possible: In the dry state, the $MPC_{x\%}$-films are very oleophilic, independent of the amount of BPO and the associated crosslinking points, indicated by the very low contact angle (less than 10°) against hexadecane (Figure 4). When the surfaces are wetted with water, it penetrates the MPC-films and they swell depending on their degree of crosslinking. The dipole arrangement of water molecules in the hydration shell formed via electrostatic interaction with the charged groups is closer to free water in comparison to the directional arrangement of water molecules in the hydration shell formed by hydrogen bonds, as in the case of the widely discussed PEG.[59] Because of this phenomenon and the low concentration of MPC chains in the swollen layer, the water film which is formed between the SiO_2 substrate and the oil droplet is behaving similar to pure water and leading to a significant decrease of the interaction between the oil droplet and the surface. Because of its lower density, the oil swims away on top of the water film.

2.4. Fouling Resistance Study

MPC polymers have been widely investigated as surface modification of various materials to avoid the adsorption of biomolecules, especially proteins, in the past decades.[30,60,61] These zwitterionic polymers have a strong hydration ability resulting

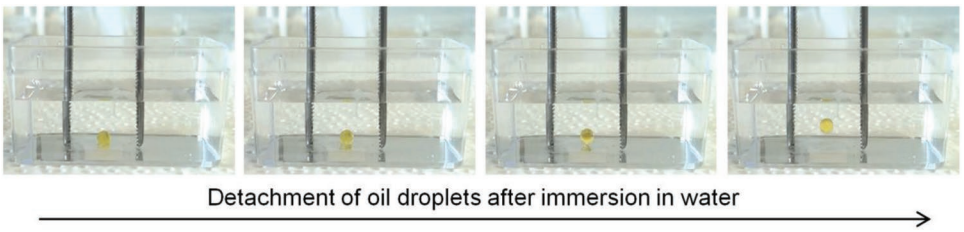

Figure 6. Representation of a typical experiment for the determination of the time of detachment of an oil droplet by immersion into pure water.

in a hydration layer bound through solvation of the charged terminal groups as described above. Furthermore, the elastic repulsion energy, describing the steric repulsion force during the interaction between protein and surface, has an influence on the protein adsorption.[61] Therefore, films of MPC-polymers are also discussed as protein-repellent surfaces and have a better antifouling performance as PEG.[62,63] Protein repellence is important for antifouling surfaces because every biofilm formation starts with the adsorption of so-called extra cellular biomolecules, like proteins or lipids, released from cells.[64,65] These molecules enhance the adsorption of cells on surfaces and feed the subsequent first layer of cells which is followed by biofilm formation. That means, for the generation of surfaces with antifouling properties the first step of biofilm formation has to be inhibited. Different studies demonstrated the reduction of the cell adhesion by MPC-polymers with different constitution previously.[30,31,34] The nonfouling behavior of MPC is a result of its strong protein-repellent properties. In this contribution we have tested the antifouling performance of the $MPC_{x\%}$ polymers depending on the amount of crosslinking. For this purpose we have investigated the cell adhesion of a Gram-negative (*Escherichia coli*) and a Gram-positive (*Bacillus subtilis*) bacteria as well as of the yeast fungus *Saccharomyces cerevisiae* to cover the behavior of different pathogens. These cells cover different adsorption mechanisms due to their membrane properties. The results of the cell adhesion studies are summarized in **Figure 7** and show the comparison between adhesions on nonfunctionalized SiO_2 with MPC-coated surfaces, crosslinked for 2 min. All images (Figure 7c,e,g as well as Section S5 in the Supporting Information) demonstrate a significant reduction of the pathogen adsorption regardless of the BPO-content of the grafted polymer. To investigate the fouling resistance in detail the illuminated pixel, induced by the staining of the adsorbed cell nuclei with a fluorescence dye, were counted and related to the dark pixel, where no cells are adsorbed (Figure 7a). It is conspicuous that the adsorption of *E. coli* on SiO_2 is approximately five times higher than that of the other two pathogens, indicating a stronger interaction of the Gram-negative bacterium with the surface. Gram-negative bacteria are characterized by a very thin single-layered peptidoglycan shell decorated with a large number of lipopolysaccharides and lipoproteins, in contrast to Gram-positive cells having a very thick murein layer with teichoic acids. It is known, that the lipopolysaccharides of Gram-negative bacteria can interact quite well with SiO_2 through hydrogen bonds of the silica surface hydroxyl groups.[66] Nevertheless, the amount of adsorbed cells of every investigated species was significantly decreased at the MPC films. However, it was also to be seen that the antifouling behavior was influenced by swelling and water contact angle of the investigated films (Figure 4a,b). As mentioned above the degree of swelling decreased and the water contact angle increased with increasing BPO content. Hence, it was found that $MPC_{1\%}$-films are more effective to repel proteins than $MPC_{4\%}$-films. It has to be mentioned, that the results in Figure 7a demonstrate a general trend because of the standard derivation which was large in relation to the small differences of the BPO-amount and the generally high effectiveness of the investigated zwitterionic phosphorylcholine films to repel proteins.

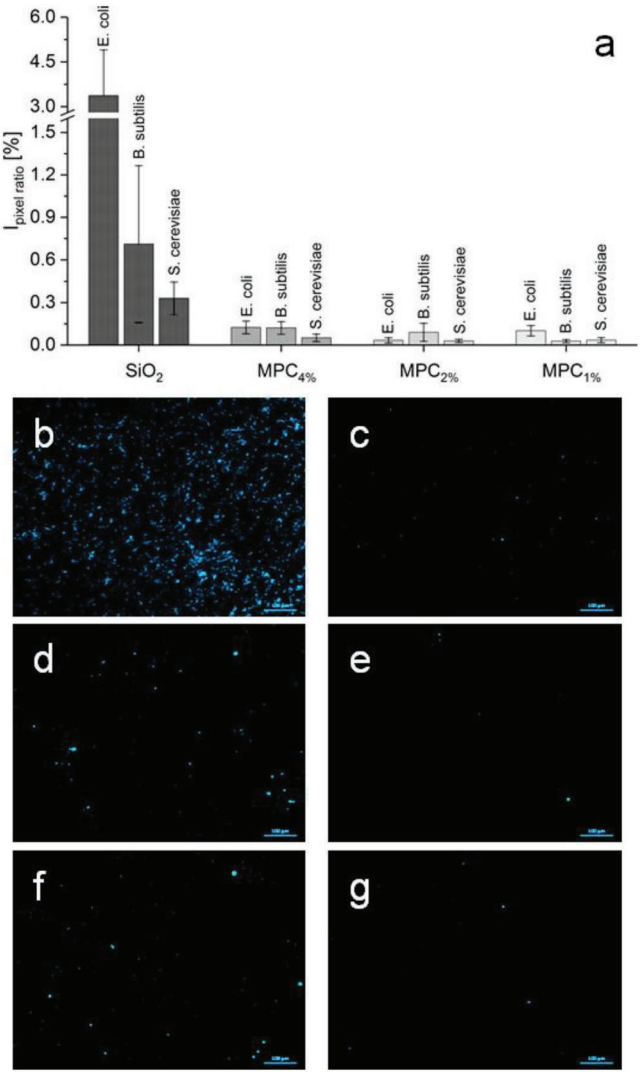

Figure 7. a) Quantitative analysis of cell adhesion experiments on MPC-polymers with different amounts of benzophenone in comparison to a pure SiO_2 surface by evaluation of the ratios between the pixels induced by the fluorescence marker of the cells and the black pixels of the surface with no adsorbed cells. b–g) Qualitative investigation of the nonfouling behavior of a $MPC_{2\%}$ functionalized silicon surface by evaluation of the adhesion of c) *E. coli*, e) *B. subtilis*, and g) *S. cerevisiae* in comparison to the adsorption on b,d,f) respective pure SiO_2 surfaces.

3. Conclusion

In this contribution the effectiveness of a multifunctional coating based on the zwitterionic and hydrophilic phosphorylcholine and photoreactive benzophenone units was demonstrated, which has simultaneously an excellent easy-to-clean, anti-fog, as well as antifouling performance and can be steadily attached. The layers were prepared by a fast single grafting-to step, whereby the films were crosslinked on the surfaces via UV-irradiation. For this, a benzophenone-containing comonomer was introduced into the polymers with low concentration. To evaluate the presented functionalities and to achieve a better understanding of structure–property relations three different copolymers with 1%, 2%, and 4% benzophenone were

Table 1. Compositions, yields, molecular weight, as well as PDI of synthesized polymers $MPC_{1\%}$, $MPC_{2\%}$, and $MPC_{4\%}$.

Polymer	[MPC]:[BPO]:[EBiB][a]	Polymer composition [MPC]:[BPO][b]	Yield	M_n [g mol^{-1}][c]	M_w [g mol^{-1}][c]	PDI[c]
$MPC_{1\%}$	198:2:1	99:1 (≙ 1% BPO)	64.9%	21 500	38 000	1.77
$MPC_{2\%}$	195:5:1	49:1 (≙ 2% BPO)	42.0%	18 250	33 250	1.82
$MPC_{4\%}$	190:10:1	431:19 (≙ 4.2% BPO)	84.4%	21 500	38 500	1.79

[a]Ratio of monomers ([MPC], [BPO]) and initiator ([EBiB]) for ATRP of MPC copolymers (reaction conditions: CuBr:bipy:EBiB = 1:2:1, 2-propanol, 0.25 mol L^{-1}, r.t., 24 h); [b]Determined by 1H NMR spectroscopy in methanol-d4; [c]Estimated by GPC.

synthesized and deposited. The study has shown that an exactly balanced ratio between thickness of the dry films, degree of swelling, and water contact angle is necessary to create surface coatings with tailored properties. The investigations show that films of MPC with a content of 1% BPO delivered optimal oil repellency. Generally, a degree of swelling of ≈15 in combination with a water contact angle of less than 12° was necessary for a reliable easy-to-clean effect. In contrast to these findings, the BPO-content has no apparent effect on the anti-fog performance. This effect could be generated independent of the polymer composition. Furthermore, the antifouling behavior was tested by cell adsorption experiments of Gram-negative (*E. coli*) and Gram-positive (*B. subtilis*) bacteria as well as of the yeast fungus *S. cerevisiae*. It was found that zwitterionic polymer layers with a BPO content of 1% to 4% are able to reduce significantly the adsorption of these pathogens and have a high antifouling capability, whereby the $MPC_{1\%}$ films show the best performance.

4. Experimental Section

Materials: Acetonitrile (≥99.8%, Sigma Aldrich), 2-butanone (≥99.5%, Sigma Aldrich), 4-hydroxybenzophenone (98%, Sigma Aldrich), triethylamine (≥99.5%, Sigma Aldrich), methacryloyl chloride (97%, ABCR), sodium hydroxide (98%, Acros Organics), sodium sulfate (≥99%, Sigma Aldrich), ethanol (100%, VWR Chemicals), dichloromethane (≥99.8%, Acros Organics), copper bromide (CuBr, 99.998%, Alfa Aesar), ethyl-2-bromoisobutyrate (EBiB, 98%, Sigma Aldrich), 2,2′-bibyridine (bipy, ≥99%, Sigma Aldrich), *n*-hexane (≥99%, Merck KGaA), 2-propanol (99.5%, Acros Organics) were used without further purification. 2-methacryloyloxyethyl phosphorylcholine (MPC; 97%, Sigma Aldrich) was purified twice by recrystallization from acetonitrile. For all purposes, if it was necessary, Millipore water was used. As substrates highly polished silicon wafers orientated in [100] direction and with ≈1.3 nm native SiO_2 were purchased from Si-Mat (Silicon Materials, Kaufering, Germany).

Synthesis: The reaction schemes of the synthesized monomer BPO and $MPC_{x\%}$ polymers are demonstrated in Scheme S1 in the Supporting Information.

Synthesis of BPO: According to the synthesis of BPO published previously,[67] 11 g (0.051 mol) 4-hydroxybenzophenone and 8.5 mL (0.05 mol) triethylamine were dissolved in 220 mL dry 2-butanone, placed under inert conditions in a three-necked flask and cooled down to a temperature of 0 °C. Afterward 5.9 mL (0.059 mol) methacryloyl chloride dissolved in 18 mL 2-butanone was added drop wise into the flask under intensive stirring in such a way that the temperature was maintained between 0 and 5 °C. Afterward the reaction mixture was stirred for 1 h at 0 °C and for another hour at room temperature. The triethylammonium chloride, which precipitated during the reaction, was filtered off and the solvent was removed by distillation. The obtained residue was diluted in diethyl ether, washed twice with 0.1% NaOH and water, and dried over anhydrous Na_2SO_4. Afterward the organic solvent was evaporated to get the crude oily product BPO. The product was redissolved in dichloromethane, dried over Na_2SO_4 again, precipitated, and purified by recrystallization from ethanol yielding in a white powder (8.3 g, 60.8%). ^{1}H-NMR (500.13 MHz, $CDCl_3$, δ): 2.01 (s, 3H, $-CH_3$), 5.72 (s, 1H, $=CH_2$), 6.31 (s, 1H, $=CH_2$), 7.19 (d, 2H, aromatic), 7.41 (q, 2H, aromatic), 7.51 (q, 1H, aromatic), 7.72 (d, 2H, aromatic), 7.80 (d, 2H, aromatic); ^{13}C-NMR (125.77 MHz, $CDCl_3$, δ): 18.3 ($-CH_3$), 127.8 ($=CH_2$), 135.6 (=C<), 121.5, 128.3, 129.9, 131.6, 132.5, 134.5, 137.5, and 154.2 (aromatic carbons), 165.3 (>C=O ester), 195.5 (>C=O ketone); FTIR-ATR (bulk material): $\tilde{\upsilon}$ (cm^{-1}) = 3513, 3449, 3373, 3293, 3103, 3050, 2990, 2927, 2849, 2744, 1920, 1763, 1730, 1650, 1596, 1578, 1499, 1446, 1408, 1379, 1344, 1318, 1302, 1276, 1198, 1160, 1148, 1121, 1096, 1041, 938, 923, 833, 805, 789, 733, 696, 678, 640.

Synthesis of Poly[(2-methacryloyloxyethyl phosphorylcholine)-co-benzophenyl methacrylate] ($MPC_{x\%}$): Copolymers composed of different ratios of the monomers MPC and BPO were synthesized following an ATRP protocol. The ratio between the initiator EBiB and the monomers was set to 1:200 in every synthesis. The exact ratios, yields, molecular weights, and polydispersity indices are summarized in **Table 1**. Copolymers with a content of 1% BPO, 2% BPO, and 4% BPO were synthesized and denoted below as $MPC_{1\%}$, $MPC_{2\%}$, and $MPC_{4\%}$. In a typical experiment 1.616 g (5.472 mmol) MPC, 4 mg (0.026 mmol) CuBr, and 8.7 mg (0.052 mmol) bipy were placed in a Schlenk flask, dissolved in 22 mL 2-propanol, and filled with argon. Because of the insolubility of BPO in alcohols, this reactant (14 mg, 0.0547 mmol) was dissolved in 0.3 mL 2-butanone and was added to the 2-propanol solution. Afterward the mixture was degassed three times by freeze-pump-thaw cycles. To start the polymerization 4 µL (0.0273 mmol) of the initiator EBiB was added at room temperature. After 24 h the reaction was stopped by air exposure and the solution was passed through a column filled by neutral alumina to remove the catalyst. The polymer was precipitated in *n*-hexane and purified by twofold precipitation from *n*-hexane. After drying under vacuum for 24 h, the polymer ($MPC_{1\%}$) was obtained as a white solid (1.058 g, 64.9%). ^{1}H-NMR (500.13 MHz, methanol-d4, δ): 0.97–1.97 (br, polymer backbone), 3.30 (br, $-N^+(CH_3)_3$), 3.74, 4.08, 4.23, and 4.33 (br, $-CH_2$ of MPC side chain), 7.41, 7.47, 7.60, 7.70, 7.82, and 7.96 (br, aromatic); ^{13}C-NMR (125.77 MHz, methanol-d4, δ): 18.2, 19.9, 20.7 (br, CH_3-backbone), 46.1, 46.4 ($C_{quaternary}$-backbone), 54.8 ($-N-CH_3$), 55.6 (br, CH_2-backbone), 60.6 ($-O-CH_2-CH_2-N-$), 64.3 ($-O-CH_2-CH_2-O-$), 66.2 ($-O-CH_2-CH_2-O-$), 67.4 (br, $-O-CH_2-CH_2-N-$), 122.6, 129.8, 131.1, 132.9, 134.1, 136.6, 138.5, and 155.2 (aromatic carbons), 178.2, 179.1, and 179.3 (>C=O), 197.3 (>C=O ketone); ^{31}P-NMR (202.46 MHz, methanol-d4, δ): –0.45 (br); FTIR-ATR (bulk material): $\tilde{\upsilon}$ (cm^{-1}) = 3343, 3034, 2957, 1717, 1657, 1599, 1480, 1405, 1342, 1232, 1163, 1054, 954, 927, 875, 852, 828, 775, 746.

Surface Modification—Cleaning of Silicon Substrates: The silicon substrates (1.3 × 2 cm^2) were purified with absolute ethanol in an ultrasonic bath twice for 10 min and dried under nitrogen flux. Then the samples were activated in an oxygen plasma chamber (Expanded Plasma Cleaner, Harrick Plasma, Ithaca, USA) for 1 min at 100 W.

Surface Modification—Grafting-to of $MPC_{x\%}$ on SiO_2: In a typical experiment the functional polymer $MPC_{x\%}$ was deposited on the purified and activated silica surfaces by spin coating (ν = 2500 r min^{-1}, a = 1000 r (min s)$^{-1}$, V = 100 µL, t_{spin} = 10 s) from a 0.5 wt% MPC solution in absolute ethanol (prefiltered using a PTFE syringe filter, pore size 0.2 µm). Afterward the polymer was grafted at room temperature by UV-irradiation (λ = 254 nm) using an UV-lamp made by Herolab (Herolab GmbH Laborgeräte, Wiesloch, Germany) with

a defined distance of 1 cm to the samples at different exposure times (30 s–11 min). After the grafting process, the excess of nonbonded polymer was removed by extraction with fresh ethanol from the silicon samples followed by drying in a steam of nitrogen.

Characterizations of Bulk Polymers, Polymer Layers, and Surfaces—NMR Spectroscopy (NMR): ^{1}H (500.13 MHz), ^{13}C (125.77 MHz), and ^{31}P (202.46 MHz) NMR spectra were recorded on an Advance III 500 spectrometer (Bruker, Germany) using $CDCl_3$ in the case of BPO and methanol-d4 as solvent and internal reference for the $MPC_{x\%}$ polymers (δ_{CDCl3} (^{1}H) = 7.27 ppm, δ_{CDCl3} (^{13}C) = 77.0 ppm, $\delta_{methanol\text{-}d4}$ (^{1}H) = 3.31 ppm, $\delta_{methanol\text{-}d4}$ (^{13}C) = 49.2 ppm).

Characterizations of Bulk Polymers, Polymer Layers, and Surfaces—Gel Permeation Chromatography (GPC):The determination of the molecular weight distribution and molecular weight of the synthesized MPC polymers was performed on an Agilent Technologies HP Agilent 110 HPLC system equipped with a refractive index detector K-2301 made by Knauer. The calibration of the measurements was performed with poly(ethylene glycol) standards. As an eluent a mixture composed of 0.05 mol L^{-1} trizma buffer (pH = 8, Sigma Aldrich) and 0.2 mol L^{-1} $NaNO_3$ solution with a flow of 1 mL min^{-1} was used in combination with one PolarGel-M column from Polymer Laboratories.

Characterizations of Bulk Polymers, Polymer Layers, and Surfaces—Attenuated Total Reflectance-Fourier Transform Infrared Spectroscopy (ATR-FTIR): To confirm the presence of the polymeric nanolayer as well as the crosslinking reaction with increasing time of irradiation on SiO_2 surfaces qualitatively, multiple ATR-FTIR spectroscopy was used.[68,69] The ATR-FTIR spectra were obtained using the FTIR spectrometer Vertex 70 (Bruker, Ettlingen, Germany) equipped with a mercury-cadmium-telluride (MCT)-detector (InfraRed Associates Inc., Stuart (FL), USA) and a multiple reflection ATR-Si-wafer unit (Bruker, Ettlingen, Germany). A float-Zone (FZ) Si-wafer of the ATR-Si-wafer unit was used both as model Si-wafer substrate to deposit the MPC films and as an ATR-crystal (40 mm long, reflection number is ≈46 to improve measurement sensitivity and signal-to-noise ratio). Conventional ATR-spectra of the bulk materials were collected using a SPECAC spectrometer (single reflection Golden Gate Diamond ATR-unit; SPECAC, Orpington, United Kingdom). The spectral range was 4000–1000 cm^{-1} in the case of thin film analysis and 4000–600 cm^{-1} for the investigation of the bulk samples with 4 cm^{-1} spectral resolution. 300 and 100 scans were co-added to every multiple and single ATR-spectrum respectively. To simplify data comparison a spectral baseline correction was implemented. The spectra were evaluated by using the OPUS software (version 7.5).

Characterizations of Bulk Polymers, Polymer Layers, and Surfaces—UV–vis Spectroscopy (UV–vis): The UV–vis spectra were collected using a Specord40 spectrometer from Analytik Jena, Germany, in the range between 190 and 500 nm with fused silica cuvettes (d = 1 cm). The pure MPC-polymer and the MPC-co-polymers were dissolved in ethanol in contrast the pure BPO-polymer, which was soluble in $CHCl_3$. The evaluation was achieved by using the Win ASPECT-software (version 2.3.1.0).

Characterizations of Bulk Polymers, Polymer Layers, and Surfaces—AFM: The surface topology of the different MPC-polymer layers deposited on SiO_2 was evaluated by a Dimension 3100 device with a NanoScope IIIa-controller from Veeco Digital Instruments (Metrology Group, USA). The microscope was operated with Si-cantilevers in the tapping mode with a resonance frequency of 273 kHz and a scan rate of 0.3 Hz. For the determination of the roughness S_q the whole area of the demonstrated images was evaluated. For evaluation and analysis the Nanoscope software (version 5.12) was used.

Characterizations of Bulk Polymers, Polymer Layers, and Surfaces—Dynamic CA Measurements: Dynamic CA measurements were performed with the optical contact angle instrument OCA40 by DataPhysics Instruments GmbH (Filderstadt, Germany). All contact angles were measured by sessile drop experiments as advancing (θ_{adv}) and receding contact angles (θ_{rec}) at 23 °C. Millipore water (surface tension = 72.8 mN m^{-1} at 23 °C) as well as *n*-hexadecane (27.5 mN m^{-1} at 23 °C) were used as test liquids. The drop profile was evaluated by the tangent leaning method.

Characterizations of Bulk Polymers, Polymer Layers, and Surfaces—Ellipsometry: For the evaluation of the thicknesses of the dry and swollen MPC polymer films on SiO_2, a spectroscopic ellipsometer (alpha-SE, Woollam Co., Inc., Lincoln NE, USA) equipped with a rotating compensator was used to measure the ellipsometric data Δ (relative phase shift) and tan ψ (relative amplitude ratio). The ratio of the swollen and dry film thickness is defined as degree of swelling. All measurements were performed between 370 and 900 nm at an angle of incidence (Φ_0) of 70°, which is close to the Brewster angle of silicon. To evaluate the refractive index n and the thickness d of the polymer films in dry state and in situ (swollen), a multilayer-box-model consisting of silicon, SiO_2, anchored polymer layer, and ambient was used. The optical constants for silicon and silicon oxide were taken from literature.[70] For the polymer layers, $n(\lambda)$ was fitted to a two parameter Cauchy equation ($n(\lambda) = A + B/\lambda^2$), whereas the extinction coefficient k is zero, describing the dependence of the refractive index on the wavelength. In the case of film thicknesses below 10 nm, the parameter A and B were fixed to constant values obtained from measurements of films with higher thicknesses (>20 nm). The data are summarized in Table S1 of the Supporting Information. For analysis of the swollen film thickness, in situ measurements were conducted in a batch cuvette (TSL Spectrosil, Hellma, Müllheim, Germany) at 23 °C that was closed with a Teflon covering.[70] All data were acquired and evaluated using the CompleteEASE software package, version 4.46.

Oil droplet Detachment Experiments: For the evaluation of the oil-removing behavior of various MPC films the oil detachment was determined. In a typical experiment a droplet of oil (V = 20 µL) was prepared on the dry surfaces. Olive oil was used as test contamination. Afterward the samples were put into clean water (Millipore, 40 mL) without tilting the surface. The time between the first contact of the surface with water and the complete detachment of the oil droplet was determined and denoted as oil detaching time. If the oil droplet could not be removed from the sample after 1 min, the experiment was interpreted as "not passed."

Anti-Fog Experiments: The anti-fog performance was investigated qualitatively by breathing on the surface for 10 s. After this time the fog formation on an MPC-functionalized surface was visually compared with a nonfunctionalized one.

Cell Adhesion Experiments: To investigate the antifouling performance of the MPC films with different contents of BPO as well as of the nonfunctionalized surfaces as control, cell adhesion experiments of *E. coli* and *B. subtilis* in S1-bouillon culture medium as well as *S. cerevisiae* in YPD-bouillon were performed. The bacteria suspensions were generated by inoculation of the nutrient media with preculture for 24 h at 30 °C in a laboratory shaker resulting in a cell number of ≈10^9 microorganisms mL^{-1}. Afterward the samples, beforehand disinfected in 70% ethanol, were immersed in a *B. subtilis* or *E. coli* suspension for 24 h and in a *S. cerevisiae* suspension for 48 h at 30 °C, respectively. To remove the nonadsorbed cells, the surfaces were subsequently washed several times with fresh phosphate buffer (0.068 mol L^{-1} KH_2PO_4–K_2HPO_4, pH = 7.0). The cell nuclei were stained by 4′,6-diamidino-2-phenylindole dihydrochloride (DAPI) as a fluorescence marker. The result of the cell adsorption was investigated by using a ZEISS ApoTome.2 fluorescence microscope after incubation in darkness for 10 min.

Supporting Information

Supporting Information is available from the Wiley Online Library or from the author.

Acknowledgements

A.S.M., S.A. and T.F. gratefully acknowledge the funding from the Federal Ministry for Economic Affairs and Energy (BMWi) of Germany (AiF-IGF 18696 BR and AiF-IGF 18573 BG/1). The authors thank Hannes

Kettner for collecting the AFM-images. Furthermore Hartmut Komber is acknowledged for the NMR-spectra, Eva Bittrich for her support regarding to the evaluation of in situ ellipsometry data and Christina Harnisch for conducting the GPC measurements. The authors thank Dr. Helfried Haufe and Annabell Radisch (Gesellschaft zur Förderung von Medizin-, Bio-und Umwelttechnologien e.V., Dresden, GMBU, Germany) for performing the cell adhesion experiments and acknowledge the great support of Dr. Helfried Haufe regarding the evaluation of the cell adhesion.

Conflict of Interest

The authors declare no conflict of interest.

Keywords

coatings, phosphorylcholines, polymer interfaces, thin films, zwitterionic polymers

Received: August 15, 2019
Revised: October 10, 2019
Published online: December 1, 2019

[1] P. Uhlmann, R. Frenzel, B. Voit, U. Mock, B. Szyszka, B. Schmidt, D. Ondratschek, J. Gochermann, K. Roths, *Prog. Org. Coat.* **2007**, *58*, 122.
[2] H. Guo, T. Xu, J. Zhang, W. Zhao, J. Zhang, C. Lin, L. Zhang, *Chem. Eng. J.* **2018**, *351*, 409.
[3] Z. Han, Z. Mu, W. Yin, W. Li, S. Niu, J. Zhang, L. Ren, *Adv. Colloid Interface Sci.* **2016**, *234*, 27.
[4] S. Zhang, J. Huang, Y. Cheng, H. Yang, Z. Chen, Y. Lai, *Small* **2017**, *13*, 1701867.
[5] K. R. Khedir, G. K. Kannarpady, C. Ryerson, A. S. Biris, *Prog. Org. Coat.* **2017**, *112*, 304.
[6] B. Liu, K. Zhang, C. Tao, Y. Zhao, X. Li, K. Zhu, X. Yuan, *RSC Adv.* **2016**, *6*, 70251.
[7] S. H. Anastasiadis, *Langmuir* **2013**, *29*, 9277.
[8] Q. Xu, W. Zhang, C. Dong, T. S. Sreeprasad, Z. Xia, *J. R. Soc., Interface* **2016**, *13*, 20160300.
[9] J. Yong, F. Chen, Q. Yang, J. Huo, X. Hou, *Chem. Soc. Rev.* **2017**, *46*, 4168.
[10] J. A. Howarter, J. P. Youngblood, *Macromol. Rapid Commun.* **2008**, *29*, 455.
[11] P. Chevallier, S. Turgeon, C. Sarra-Bournet, R. Turcotte, G. Laroche, *ACS Appl. Mater. Interfaces* **2011**, *3*, 750.
[12] Y. Wang, Q. Dong, Y. Wang, H. Wang, G. Li, R. Bai, *Macromol. Rapid Commun.* **2010**, *31*, 1816.
[13] I. Banerjee, R. C. Pangule, R. S. Kane, *Adv. Mater.* **2011**, *23*, 690.
[14] S. Krishnan, C. J. Weinman, C. K. Ober, *J. Mater. Chem.* **2008**, *18*, 3405.
[15] D. M. Yebra, S. Kiil, K. Dam-Johansen, *Prog. Org. Coat.* **2004**, *50*, 75.
[16] T. Goda, K. Ishihara, Y. Miyahara, *J. Appl. Polym. Sci.* **2015**, *132*, n/a.
[17] N. Nakabayashi, Y. Iwasaki, *Bio-Med. Mater. Eng.* **2014**, *14*, 345.
[18] A. V. Fuchs, S. Ritz, S. Pütz, V. Mailänder, K. Landfester, U. Ziener, *Biomater. Sci.* **2013**, *1*, 470.
[19] M. Ayaki, A. Iwasawa, Y. Niwano, *Jpn. J. Ophthalmol.* **2011**, *55*, 541.
[20] M. Kobayashi, K. Ishihara, A. Takahara, *J. Biomater. Sci., Polym. Ed.* **2014**, *25*, 1673.
[21] M. Koji, L. Y. Norifumi, S. Hidenori, S. Hideki, T. Naoya, S. Tsukasa, F. Michihiro, T. Atsushi, *J. Phys.: Conf. Ser.* **2011**, *272*, 012017.
[22] N. A. Krylov, V. M. Pentkovsky, R. G. Efremov, *ACS Nano* **2013**, *7*, 9428.
[23] M. L. Berkowitz, R. Vácha, *Acc. Chem. Res.* **2012**, *45*, 74.
[24] T. Morisaku, J. Watanabe, T. Konno, M. Takai, K. Ishihara, *Polymer* **2008**, *49*, 4652.
[25] Y. Xu, M. Takai, K. Ishihara, *Ann. Biomed. Eng.* **2010**, *38*, 1938.
[26] R. Matsuno, K. Ishihara, *Nano Today* **2011**, *6*, 61.
[27] Q. Liu, J. Locklin, *ACS Omega* **2018**, *3*, 17743.
[28] A. S. Münch, A. Stake, T. Lukasczyk, A. Stalling, T. Fritzsche, V. Stenzel, P. Uhlmann, *J. Coat. Technol. Res.* **2019**, https://doi.org/10.1007/s11998-019-00189-3.
[29] K. Ishihara, H. Nomura, T. Mihara, K. Kurita, Y. Iwasaki, N. Nakabayashi, *J. Biomed. Mater. Res.* **1998**, *39*, 323.
[30] A. S. Münch, M. Wölk, M. Malanin, K.-J. Eichhorn, F. Simon, P. Uhlmann, *J. Mater. Chem. B* **2018**, *6*, 830.
[31] A. S. Münch, T. Fritzsche, H. Haufe, P. Uhlmann, *J. Coat. Technol. Res.* **2018**, *15*, 703.
[32] G. Xu, P. Liu, D. Pranantyo, L. Xu, K.-G. Neoh, E.-T. Kang, *Ind. Eng. Chem. Res.* **2017**, *56*, 14479.
[33] A. L. Lewis, *Colloids Surf., B* **2000**, *18*, 261.
[34] Q. Liu, P. Singha, H. Handa, J. Locklin, *Langmuir* **2017**, *33*, 13105.
[35] W. Jiang, G. Fischer, Y. Girmay, K. Irgum, *J. Chromatogr. A* **2006**, *1127*, 82.
[36] C. Xiong, J. Yuan, Z. Wang, S. Wang, C. Yuan, L. Wang, *J. Chromatogr. A* **2018**, *1546*, 56.
[37] K. He, H. Duan, G. Y. Chen, X. Liu, W. Yang, D. Wang, *ACS Nano* **2015**, *9*, 9188.
[38] I. Y. Ma, E. J. Lobb, N. C. Billingham, S. P. Armes, A. L. Lewis, A. W. Lloyd, J. Salvage, *Macromolecules* **2002**, *35*, 9306.
[39] Y. Ma, Y. Tang, N. C. Billingham, S. P. Armes, A. L. Lewis, A. W. Lloyd, J. P. Salvage, *Macromolecules* **2003**, *36*, 3475.
[40] G. Dormán, H. Nakamura, A. Pulsipher, G. D. Prestwich, *Chem. Rev.* **2016**, *116*, 15284.
[41] M. Marazzi, S. Mai, D. Roca-Sanjuán, M. G. Delcey, R. Lindh, L. González, A. Monari, *J. Phys. Chem. Lett.* **2016**, *7*, 622.
[42] A. A. Lin, V. R. Sastri, G. Tesoro, A. Reiser, R. Eachus, *Macromolecules* **1988**, *21*, 1165.
[43] J. D. J. S. Samuel, T. Brenner, O. Prucker, M. Grumann, J. Ducree, R. Zengerle, J. Rühe, *Macromol. Chem. Phys.* **2010**, *211*, 195.
[44] C. Bunte, J. Rühe, *Macromol. Rapid Commun.* **2009**, *30*, 1817.
[45] C. Bunte, O. Prucker, T. König, J. Rühe, *Langmuir* **2010**, *26*, 6019.
[46] T. Brandstetter, S. Böhmer, O. Prucker, E. Bissé, A. zur Hausen, J. Alt-Mörbe, J. Rühe, *J. Virol. Methods* **2010**, *163*, 40.
[47] C. A. Naumann, O. Prucker, T. Lehmann, J. Rühe, W. Knoll, C. W. Frank, *Biomacromolecules* **2002**, *3*, 27.
[48] O. Prucker, C. A. Naumann, J. Rühe, W. Knoll, C. W. Frank, *J. Am. Chem. Soc.* **1999**, *121*, 8766.
[49] R. Toomey, D. Freidank, J. Rühe, *Macromolecules* **2004**, *37*, 882.
[50] J. Pahnke, J. Rühe, *Macromol. Rapid Commun.* **2004**, *25*, 1396.
[51] B. Leshem, G. Sarfati, A. Novoa, I. Breslav, R. S. Marks, *Luminescence* **2004**, *19*, 69.
[52] X. Lin, K. Fukazawa, K. Ishihara, *ACS Appl. Mater. Interfaces* **2015**, *7*, 17489.
[53] M. Toshiyuki, F. Koji, U. Koshin, *WO2006070876 (A1)*, **2006**.
[54] C. Rouns, J. Perrault, *WO2004060427 (A1)*, **2004**.
[55] V. P. Dhende, S. Samanta, D. M. Jones, I. R. Hardin, J. Locklin, *ACS Appl. Mater. Interfaces* **2011**, *3*, 2830.
[56] G. T. Carroll, M. E. Sojka, X. Lei, N. J. Turro, J. T. Koberstein, *Langmuir* **2006**, *22*, 7748.
[57] Z. Kolarova Raskova, P. Stahel, J. Sedlarikova, L. Musilova, M. Stupavska, M. Lehocky, *Materials* **2018**, *11*, 1451.
[58] L. Richert, F. Boulmedais, P. Lavalle, J. Mutterer, E. Ferreux, G. Decher, P. Schaaf, J.-C. Voegel, C. Picart, *Biomacromolecules* **2004**, *5*, 284.

[59] P. Singha, J. Locklin, H. Handa, *Acta Biomater.* **2017**, *50*, 20.
[60] K. Ishihara, N. P. Ziats, B. P. Tierney, N. Nakabayashi, J. M. Anderson, *J. Biomed. Mater. Res.* **1991**, *25*, 1397.
[61] Y. Inoue, T. Nakanishi, K. Ishihara, *Langmuir* **2013**, *29*, 10752.
[62] W. Feng, X. Gao, G. McClung, S. Zhu, K. Ishihara, J. L. Brash, *Acta Biomater.* **2011**, *7*, 3692.
[63] W. J. Yang, T. Cai, K.-G. Neoh, E.-T. Kang, S. L.-M. Teo, D. Rittschof, *Biomacromolecules* **2013**, *14*, 2041.
[64] G. O'Toole, H. B. Kaplan, R. Kolter, *Annu. Rev. Microbiol.* **2000**, *54*, 49.
[65] D. Monroe, *PLoS Biol.* **2007**, *5*, e307.
[66] L. B. Capeletti, L. F. de Oliveira, K. de A. Gonçalves, J. F. A. de Oliveira, Â. Saito, J. Kobarg, J. H. Z. dos Santos, M. B. Cardoso, *Langmuir* **2014**, *30*, 7456.
[67] S. Nanjundan, C. S. Unnithan, C. S. J. Selvamalar, A. Penlidis, *React. Funct. Polym.* **2005**, *62*, 11.
[68] E. Karabudak, R. Kas, W. Ogieglo, D. Rafieian, S. Schlautmann, R. G. H. Lammertink, H. J. G. E. Gardeniers, G. Mul, *Anal. Chem.* **2013**, *85*, 33.
[69] H. Schumacher, U. Künzelmann, B. Vasilev, K.-J. Eichhorn, J. W. Bartha, *Appl. Spectrosc.* **2010**, *64*, 1022.
[70] C. Werner, K. J. Eichhorn, K. Grundke, F. Simon, W. Grählert, H. J. Jacobasch, *Colloids Surf. A* **1999**, *156*, 3.